Sixth International Symposium on Marine Propulsors
smp'19, Rome, Italy, May 2019

Development of Supercavitation over a Body in a Duct Flow

Lotan Arad Ludar, Alon Gany

Faculty of Aerospace Engineering, Technion - Israel Institute of Technology, Haifa, Israel

ABSTRACT

Understanding the development and geometry of a supercavitation bubble is essential for the design of supercavitational vehicles as well as for prediction of bubble formation within machinery-related duct flows. The role of cavitator (nose) of a body within the flow is of major interest. To enhance insight on the supercavitation bubble development, experiments have been conducted on cylindrical slender bodies (3 mm diameter) within a duct (20 mm diameter) at different water flow velocities. A comparison of supercavitation bubbles, created on bodies with different nose geometries, has been made. The comparison referred to the conditions of the bubbles' creation and collapse, as well as on their shape and development. Various stages of the bubble development were examined for different cavitators (flat, spherical, and conical nose). Some of the experiments have been compared to numerical calculations (CFD), showing a good agreement regarding the bubble shape. It was found that the different cavitators produce similar bubble geometries, though at different flow velocities. The bubble appeared at the lowest velocity for the flat nose, then for the spherical nose, and at the highest velocity for the conical cavitator. In addition, a hysteresis phenomenon was observed, showing different bubble development paths for increasing versus decreasing the water flow velocity.

Keywords

Supercavitation, supercavities, cavitator, hysteresis.

1 INTRODUCTION

The geometry of supercavitation bubbles has been studied for decades, using diverse tools and methods, because of its significance for the design of supercavitation vehicles and applications. In particular, comprehensive researches have examined axisymmetric supercavition bubbles, proposing methods of calculation and presenting relations between the bubble dimensions and the flow conditions (Lugvinovich & Serebryakov 1975, Serebryakov 1990, Semenenko 2001, Serebryakov 2002, and others). Other studies have analyzed the wall effect in channels on the bubble dimensions as well as the values of the cavitation number of fully developed cavitation bubbles (Wu & Whitney 1971). These studies are significant for hydraulic machinery in which the appearance and development of cavitation play a key role in the performance of the system. One of the most significant topics in the field is the role of the cavitator in determining the bubble shape and size. This has been examined analytically for 2D flows (Fridman & Achkinadze 2001), and numerically for 3D flows for more accurate results and for specific geometries (Kirschner, Chamberlin & Arzoumanian 2009). Also, some estimations and predictions have been done for unbounded bubbles (Brennen 1969, Kinnas 1998, Scardoveli & Zaleski 1999, and Vasin 2001), (Shi, Wen, Zhu & Chen 2018). Other experimental investigations have described the bubbles formed on different bodies, examining the gravitation effect, the closing modes, and more. Many of them are summarized at Franc & Michel (2004).

In the present study, we investigate supercavitation bubble development over bodies in a duct water flow. We examine experimentally the influence of different cavitator geometries on axisymmetric cylindrical bodies, finding the relations between the dimensions of the bubble and the cavitation number. We have also revealed and investigated a hysteresis phenomenon in naturally developed supercavitation bubbles. Previous studies have discussed this phenomenon for ventilated (artificial) bubbles. Semenenko (2001) has examined hysteresis found in bubbles closing on a solid body, investigating the angel of the bubble closure on the solid surface as well as the required gas supply to the bubble for maintaining its size. Wosnik & Arndt (2009) have examined hysteresis for different bodies in ventilated bubbles. In our research, we observed hysteresis in bubbles that do not close on a solid body.

2 PROBLEM DESCRIPTION

We have considered axisymmetric supercavitation bubbles developing along a cylindrical object in a uniform flow of water within a convergent-divergent nozzle. Slender cylindrical bodies with different nose (cavitator) geometries have been examined. The front edge nose

causes velocity change, flow separation, and pressure drop. When the pressure decreases below the equilibrium vapor pressure of the liquid, the water starts two evaporate, developing a supercavitation bubble over the body. As the flow velocity increases, the pressure decreases, and the bubble grows and can envelope the entire body (see Fig. 1). The geometry of the body, and especially its front edge, is the main factor that determines the flow field and the supercavitation bubble creation and development.

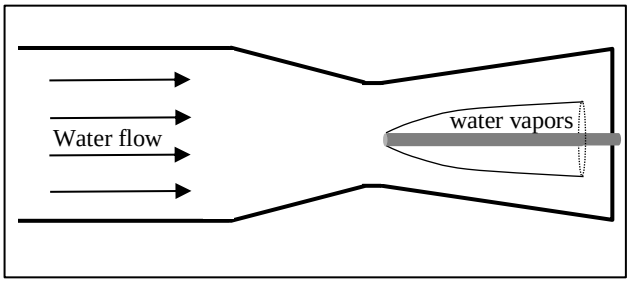

Figure 1: a scheme of the physical problem

3 THE EXPERIMENTAL SYSTEM

The experimental system included a convergence-divergence nozzle, connected to a straight pipe from which the water flew uniformly in a constant temperature of about 20°C (Fig. 2). The nozzle accelerated the flow to the appropriate speed in which cavitation could be created. A valve was used to adjust the water flow rate. The supercavitation body was placed right after the nozzle throat (Fig. 3). Three slender cylindrical bodies of 2.97 mm diameter with different cavitators (noses) have been tested: a flat cavitator, a spherical cavitator, and a conical cavitator with an angle of 15° (Fig. 4). The bubble created over the body was examined with the increase of the flow rate. Seven pressure measurement taps were placed along the wall: one at the wall of the pipe before the entrance to the nozzle, two at the converging section of the nozzle; one at the nozzle throat, where the cavitator nose was placed (the place in which we would expect to see the initial creation of the cavitation bubble); and three additional gauges at the diverging section, along the supercavitation bubble (see again Fig. 3).

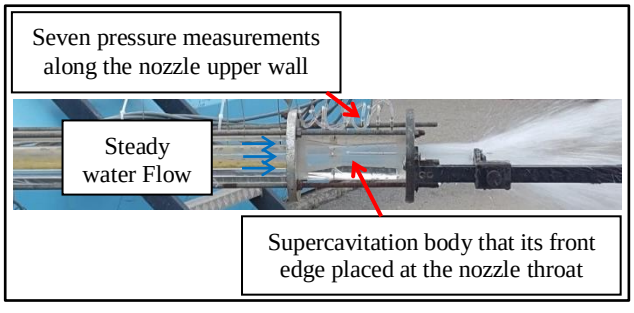

Figure 2: The experimental system

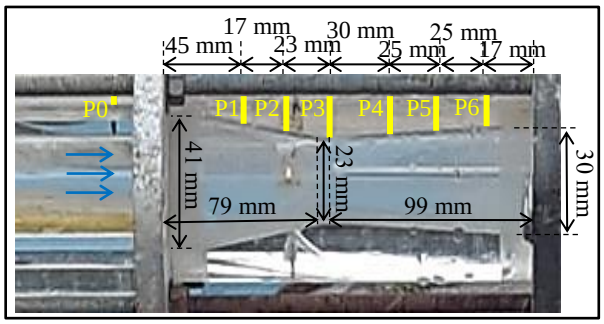

Figure 3: The nozzle geometry and the pressure measurement locations

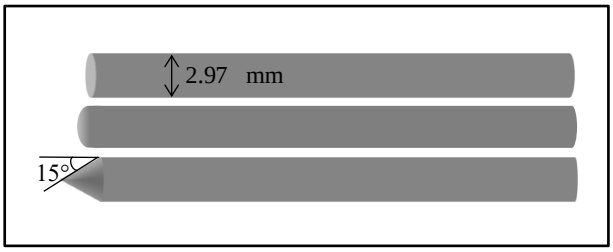

Figure 4: The supercavitation bodies

4 RESULTS

4.1 The Bubble Stages of Development

The different stages in the bubble development along the body with increasing the flow velocity are presented in Fig. 5 for the flat cavitator. The observed geometries of the bubbles were practically similar for the three different cavitators. In every stage of the flow, the bubble did not close on the body, and it remained open in its back edge. At low velocities, the geometry of the bubble surface could be expressed by the function described in equation (1):

$$f_a = \frac{d}{2}\left(1+\frac{6}{d}z\right)^{\frac{1}{3}} \quad (1)$$

where d = the cavitator diameter; z = the coordinate of the axis of symmetry.

When increasing the velocity, the function convexity changed, and the geometry of the bubble surface could be expressed by the function described in equation (2):

$$f_b = \frac{d}{2}(1+az)^{\frac{1}{2}} \quad (2)$$

where a = a constant factor, depending on the geometry of the nozzle and of the body.

When the velocity was further increased, the geometry of the bubble surface could almost be described as an open cone, with the function in equation (3):

$$f_c = \frac{d}{2}(1+az) \quad (3)$$

In general, the convexity of the bubble decreases as the velocity increases in its front and in its back edges together. Although the stages of development are similar for all three cavitators, the velocity at which the bubble starts as well as the characteristic velocity for each stage of development

are different for the different cavitators. Table 1 presents the velocities of the flow at the front edge of the cavitator for the three cavitators in the first six stages of the bubble development.

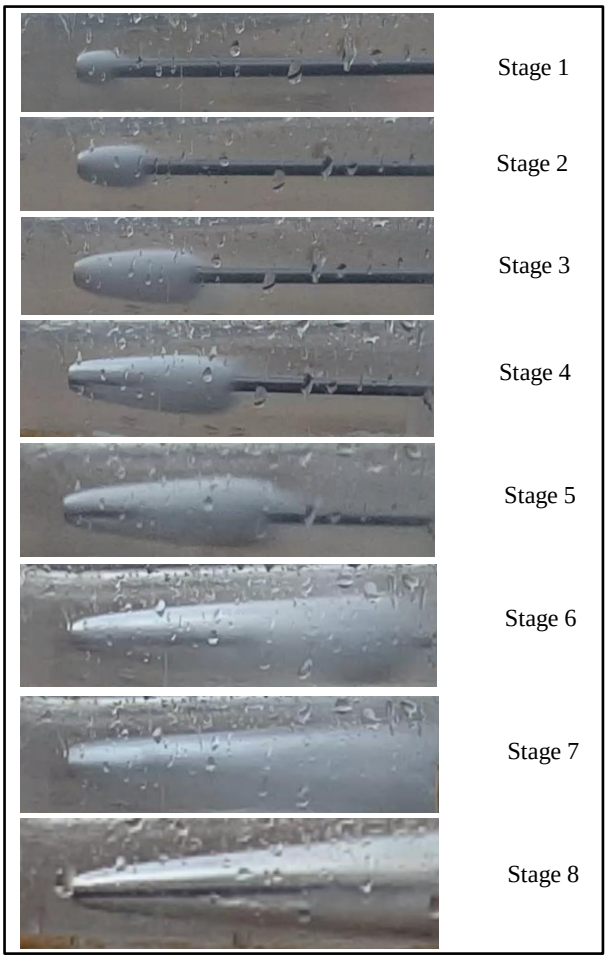

Figure 5: Stages of the bubble development for a flat cavitator

Table 1: Flow velocity at the front edge of the cavitator in stages 1 - 6 of the bubble development for the three cavitators

	Conical cavitator	Spherical cavitator	Flat cavitator
Stage 1	14.8 m/s	13.5 m/s	9.9 m/s
Stage 2	16.4 m/s	15.8 m/s	11.7 m/s
Stage 3	17.2 m/s	16.8 m/s	13.8 m/s
Stage 4	17.8 m/s	17.3 m/s	15.5 m/s
Stage 5	19.7 m/s	18.3 m/s	17.7 m/s
Stage 6	20.7 m/s	19.8 m/s	18.8 m/s

4.2 The Pressure Field

The change in the pressure has been measured on the nozzle walls. The pressure decreases moderately with the increase of the flow velocity for each of the cavitators. A rapid decrease is detected when the cavitation bubble grows and extends, reaching the section of the gauge. Similar to the order that the beginning of the bubble creation appears, the process takes place at the lowest velocity for the flat cavitator, then for the spherical cavitator and finally at the highest velocity for the conical cavitator (see measurements of P5 located at the divergent part of the nozzle where the bubble extends in Fig. 6).

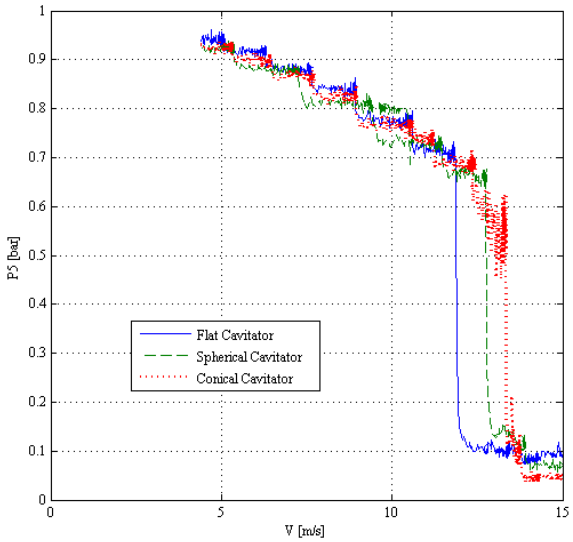

Figure 6: The wall pressure vs the velocity in P5 for the three cavitators

The results of the measurements of P5 show that there are pressure fluctuations in the system. The largest fluctuations occur for the conical cavitator, where the system is the least stable, undergoing mechanical vibrations caused by the high flow rate in the pipe required for the creation and development of the supercavitation bubble. The lowest fluctuations in the graph appear for the flat cavitator in which the bubble is created and developed in the lowest flow velocities. The lowest static wall pressure (the same for the three cavitators) measured by P4 and P5, was 0.065 and 0.07 bar (with an uncertainty of +/- 0.025 bar), respectively. These values were somewhat higher than the theoretical equilibrium vapor pressure (0.023 bar at 20°C), presumably existing within the cavitation bubble. The magnitude of the pressure drop was similar for all cavitators. Also, the pressure change was similar in all cavitators for every stage of the bubble development.

Based on the experiments, a relation between the supercavitation bubble dimensions and the cavitation number of the flow has been deduced for all three cavitators (see Fig. 7), according to equation (4):

$$l/c = A\sigma^{n} \tag{4}$$

where l = the bubble length, c = the diameter of the body, A, n = constants depending on the flow conditions, bubble position and form, and σ = the cavitation number of the flow calculated according to equation (5):

$$\sigma = \frac{p_a - p_v}{\frac{1}{2}\rho v^2} \tag{5}$$

where p_a = the atmospheric pressure, p_v = the vapor

pressure of the water, ρ = the water density, v = the water velocity.

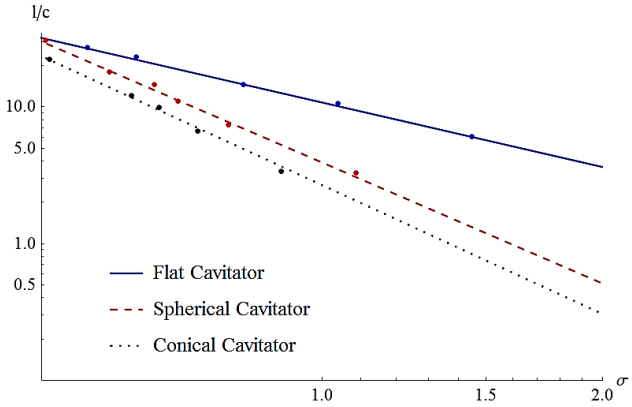

Figure 7: The measured supercavitation bubble dimension ratio vs. the cavitation number for the three cavitators

4.3 CFD

The analytical and experimental results have been compared to computational fluid dynamics (CFD) simulations using ANSYS CFX for different flow velocities \ flow rates. All simulations were steady, axisymmetric, incompressible, RANS (Reynolds Average Navier-Stokes) based with shear stress transport (SST) turbulence model and homogenous mixture multiphase flow model. Cavitation phenomena modeling for bubble generation and depletion was based on the Rayleigh-Plesset model, whereas Volume-of-Fluid (VOF) method was used for capturing the interface between the liquid and vapor phases.

The numerical calculations have shown a good agreement with the experimental results regarding the bubble shape and structure. Comparison is displayed in Fig. 8 for the flat cavitator. The stages of the bubble development appear similar.

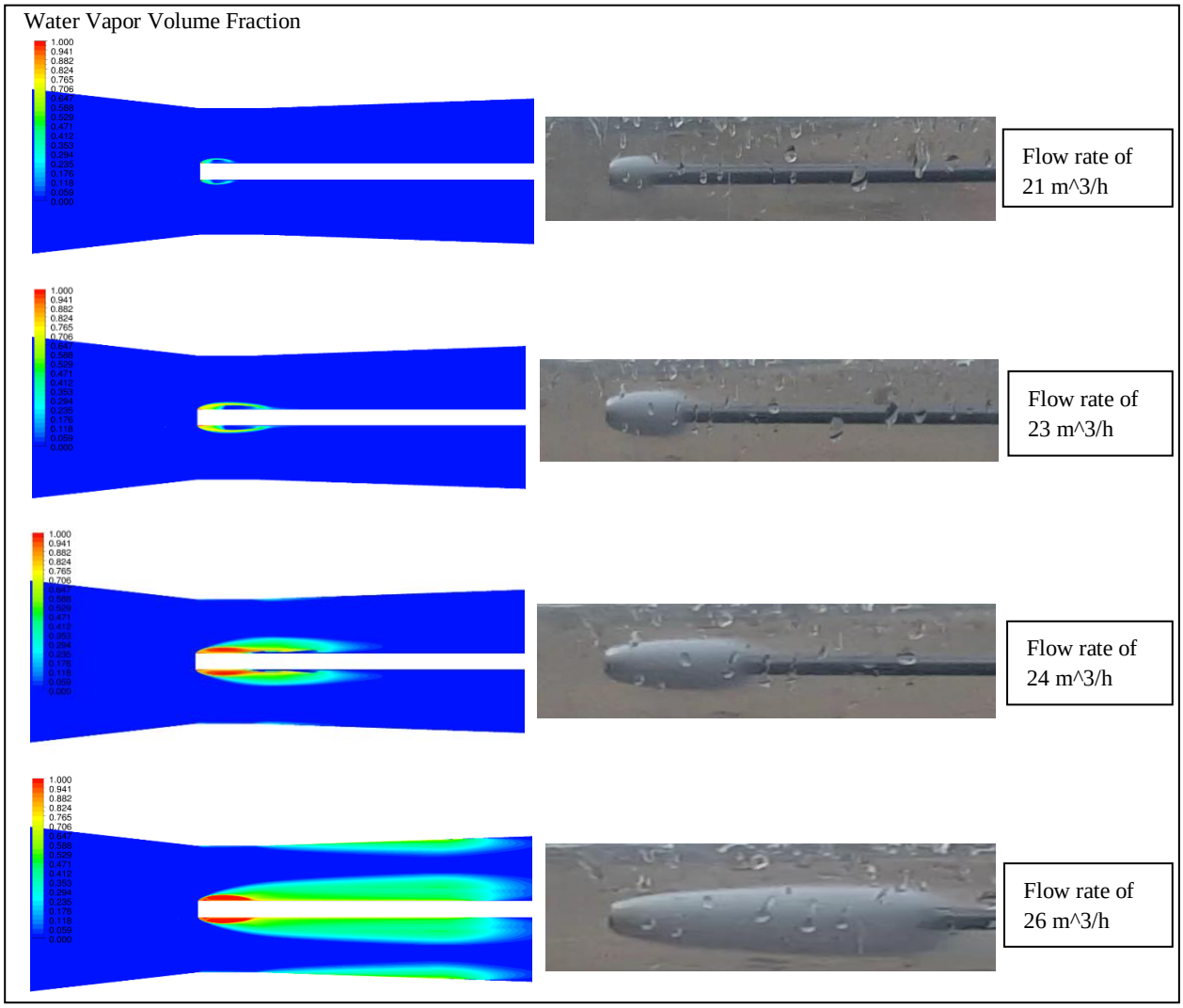

Figure 8: Experimental results and CFD simulations of the bubble development on a body with a flat cavitator

5 "HYSTERESIS"

Increasing the flow rate, the bubble grew and extended along the body until it reached the rear edge of the nozzle, which was open to the atmosphere. When opening to the atmosphere, the pressure measured at the wall grew rapidly becoming equal to the outside pressure (one atmosphere). Further increase of the flow rate did not change the pressure. Examining the situation when gradually decreasing the water flow rate revealed that initially the pressure stayed constant and the bubble had the same size and shape. Further decrease in the flow rate, dropping the flow velocity much below the value that initially caused the bubble creation, led to a sudden collapse of the bubble. Detecting the bubble size and shape as well as the wall pressure during the process, one could see a hysteresis-like phenomenon, although the physical processes were not utterly reversed. Figure 9 shows the different paths of P5 and P6 wall pressure variation for the spherical cavitator, for the two parts of the experiment (a velocity increase followed by a velocity decrease). The first part of the experiment revealed a gradual pressure decrease followed by a substantial drop, when the bubble reached the gauge section (as described in section 4.2); then an abrupt increase to the atmospheric pressure when reaching the nozzle exit. In the second part of the experiment, when decreasing the flow velocity, the bubble and the pressure remained steady until the bubble collapsed (with only a little change in pressure).

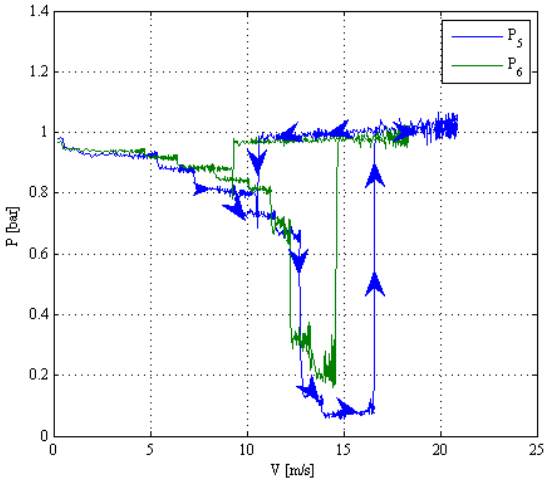

Figure 9: The wall pressure at the diverging part of the nozzle vs the velocity for the spherical cavitator during a cycle including an increase followed a decrease of the flow velocity.

6 SUMMARY

Development of a supercavitation bubble on an object in a duct flow, is affected by the walls that have a major influence on the flow regime. The cavitator role in determining the bubble shape and dimensions becomes significantly smaller and its main impact is on the conditions (flow rate \ velocity) of the bubble creation and collapse. Nevertheless, it was found that different cavitators could produce similar bubble geometries, though at somewhat different flow velocities. Testing three different cavitators at the same flow conditions and examining the bubble development for each of the cavitators, one observes that a supercavitation bubble is created at the lowest flow velocity by a cavitator generating the largest disturbance in the flow, implying a more rapid change in the flow regime. This was the flat cavitator for which the bubble was created at a velocity of only 9.9 m/s. Bubble created at the highest flow velocity occurred for the cavitator causing the least and more moderate disturbance in the flow. This was the conical cavitator, for which the bubble was created at a velocity of 14.8 m/s (50 present larger than for the flat cavitator). Another phenomenon observed was hysteresis. When increasing and decreasing the flow rates the bubble as well as the pressure variations of growth and decrease underwent through different paths. Supercavitation is a fluid dynamics phenomenon, depending mainly on the flow and pressure fields. The water quality, such as salt concentration (seawater vs. tap water), may have a small effect through the dependence of the vapor pressure. The vapor pressure of saline water is slightly lower than for pure water. For instance, at 20 degrees Celsius, vapor pressure of pure water is 0.0234 bar, and that of seawater is 0.0229 bar. This small difference would practically not change the results but might cause a little change in the velocity value for each stage of supercavitation bubble development.

REFERENCES

Brennen, C. (1969). 'A numerical solution of axisymmetric cavity flows'. Journal of Fluid Mechanics **37(4), 671-688**.

Franc, J. P., Michel, J. M. (2004). Fundamentals of Cavitation, Kluwer Academic Publishers Dordrecht**.**

Fridman, G. M., & Achkinadze, A. S. (2001). 'Review of theoretical approaches to nonlinear supercavitating flows'. Saint Petersburg State Marine Technical University, Ship Theory Department, Russia.

Kinnas, S.A. (1998). 'The prediction of unsteady sheet cavitation'. Proceedings of the 3rd International Symposium on Cavitation, Grenoble, France.

Kirschner, I. I., Chamberlin, R., & Arzoumanian, S. (2009). 'A simple approach to estimating three-dimensional supercavitating flow fields'. Proceedings of the 7th International Symposium on Cavitation CAV2009, Ann Arbor, Michigan, USA.

Logvinovich, G. V. & Serebryakov, V. V. (1975). 'On methods of calculating a shape of slender axisymmetric cavities', Hydromechanics **32, 47-54**.

Scardovelli, R., & Zaleski, S. (1999). 'Direct numerical simulation of free-surface and interfacial flow'. Annual review of fluid mechanics **31(1), 567-603**.

Semenenko, V. N. (2001). 'Artificial Supercavitation. Physics and Calculation', Proceeding of RTO Lecture Series 005 on Supercavitating Flows, Brussels, Belgium.

Serebryakov, V. V. (1990). 'Asymptotic solutions of axisymmetric problems of the cavitational flow under slender body approximation', Hydrodynamics of High Speeds, Chuvashian State University, **99-111**

Serebryakov, V. V. (2002). 'The models of the supercavitation prediction for high speed motion in water'. Proceedings of International Scientific School: HSH-2002, Chebocsary, Russia.

Shi, H. H., Wen, J. S., Zhu, B. B., & Chen, B. (2018). 'Numerical simulation of the effect of different object nose shapes on hydrodynamic process in water entry'. Proceeding of the 10th International Symposium on Cavitation, CAV2018, Baltimore, Maryland, USA.

Vasin, A. D. (2001). 'The principle of independence of the cavity sections expansion (Logvinovich's principle) as the basis for investigation on cavitation flows', Central Aerodynamics Institute (TSAGI), Moscow, Russia.

Wosnik, M. & Arndt, R. E. A. (2009). 'Control experiments with a semi-axisymmetric supercavity and a supercavity-piercing fin', Proceedings of the 7th International Symposium on Cavitation, Ann Arbor, Michigan, USA.

Wu, T. Y. T., Whitney, A. K., & Brennen, C. (1971). 'Cavity-flow wall effects and correction rules', Journal of Fluid Mechanics **49(2), 223-256**.